MODELING OF THE BEHAVIOR OF AC UNDERVOLTAGE RELAYS DURING VOLTAGE DIPS

Frederik D'hulster ; Kurt Stockman ; Jan Desmet
Hogeschool West-Vlaanderen dept. PIH
Graaf Karel de Goedelaan 5
B-8500 KORTRIJK (Belgium)
dhulsterf.pih@hogeschool-wvl.be

Ronnie Belmans
KU Leuven dept ESAT
Kasteelpark Arenberg 10
B-3001 LEUVEN (Belgium)
ronnie.belmans@kuleuven.esat.ac.be

ABSTRACT

This paper proposes a dynamic model for the behavior of an AC undervoltage protection relay during voltage dips. The behavior is expressed by means of standardized voltage tolerance curves and highly depends on the point-on-wave (phase angle) of the dip initiation. Using the model, it can be explained that AC undervoltage relays are much more sensitive to voltage dips of e.g. 50% U_{rated} than to short interruptions (0% U_{rated}), caused by the magnetic behavior. The model takes into account the electrical, magnetic and mechanical system equations. An experimental set-up with a programmable power source as dipgenerator is build to validate the model. Finally, a complete weaving machine is represented to analyze the influence towards voltage dip immunity by adding an undervoltage protection relay.

KEY WORDS: power quality analysis, voltage dips, undervoltage relay, modeling.

1. INTRODUCTION

Undervoltage relays are widely used in combination with motor circuit breakers, in order to protect both operator and load after a supply voltage interruption. To understand the behavior of the undervoltage relay during voltage dips and short interruptions, the electromagnetic equations must be analysed. A linear model is build in Matlab®/Simulink and solved by a discrete solver. Previous papers ([1], [3], [4], [5]) have described models for AC contactors but do not express the behavior using voltage tolerance curves. Voltage tolerance curves are a very useful tool to express the voltage dip immunity of complete systems or system components [2]. Voltage tolerance curves of different machine components can be superposed to define the global machine immunity.

2. VOLTAGE DIPS

A voltage dip is an instantaneous reduction of the rms voltage at a customer position. Bollen [6] characterises a voltage dip by its magnitude and duration (Fig. 1), using

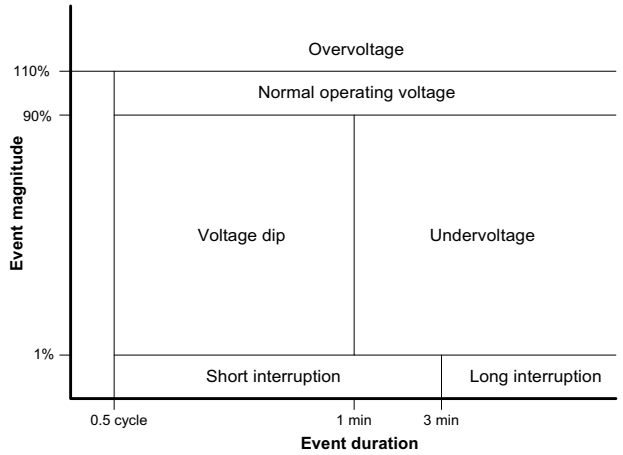

Fig. 1 Classification of voltage magnitude events (EN50160)

the EN 50160 standard. The voltage dips are either coming from the supplying high voltage system, caused by faults in the utility distribution system or generated at the users sites, connected to the distribution system. They affect all facilities linked to the same distribution network. In order to represent the immunity of system components to voltage dips and short interruptions, voltage tolerance curves are used ([6], [2]). A voltage tolerance curve divides the dip magnitude - duration plane in a ride-through (pass) and a trip (fail) area. Fig. 2 shows an example of a voltage tolerance curve of a variable speed drive.

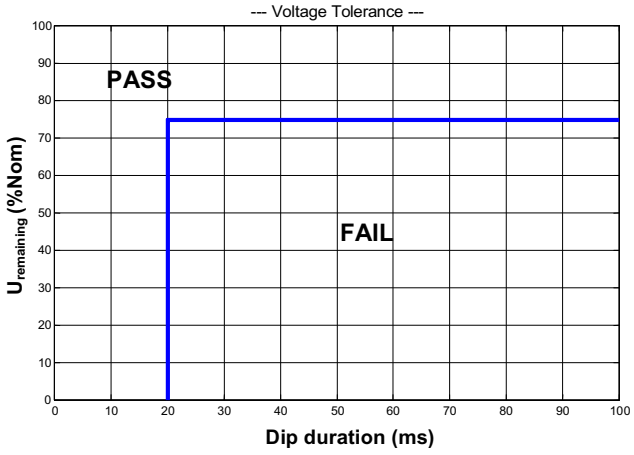

Fig. 2 Typical voltage tolerance curve for a variable speed drive

3. MODEL AND EQUATIONS

Fig. 3 shows the geometry of the modeled AC undervoltage relay. It consists of a main coil (N_1 turns) which is supplied by a voltage u_1. A shading ring with induced current i_2 is added to smoothen the magnetic force to avoid doubled frequency vibration. The magnetic flux Φ_2 has a phase shift in relation to Φ_1 and Φ_3 which realizes this damping.

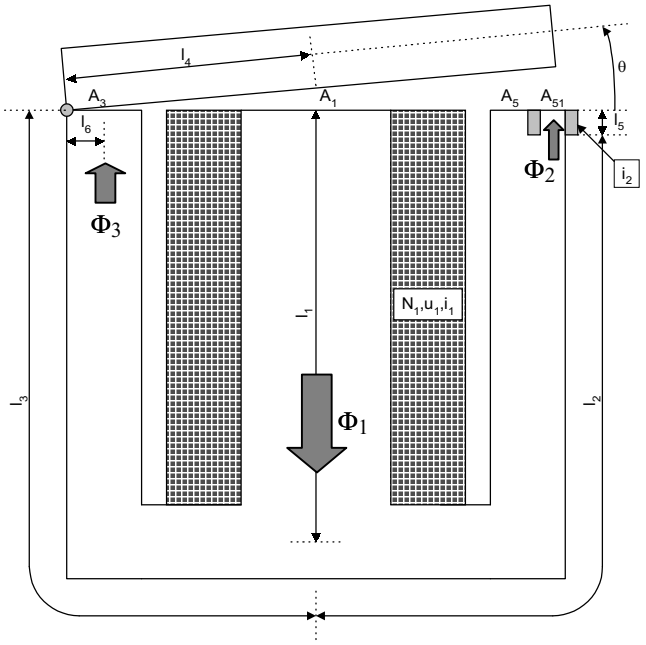

Fig. 3 Undervoltage relay geometry

The voltage equations can be written as:

$$\begin{cases} u_1 = R_1 . i_1 + N_1 . \dfrac{d\Phi_1}{dt} \\ 0 = R_2 . i_2 + \dfrac{d\Phi_2}{dt} \end{cases} \quad (1)$$

in which R_1 and R_2 are the resistances of the main and shading coil.

An equivalent magnetic circuit (Fig. 4) can be drawn with a set of constant ($\Re_i$) and position dependant ($\Re_{\theta i}$) reluctances. Using Kirchoff's law, a set of magnetic equations can be deducted:

$$\begin{cases} N_1 . i_1 = (\Re_1 + \Re_{\theta 4}).\Phi_1 + (\Re_3 + \Re_{\theta 3} + \Re_4).\Phi_3 \\ i_2 = (\Re_{51} + \Re_{\theta 51}).\Phi_2 - (\Re_3 + \Re_{\theta 3} + \Re_4).\Phi_3 \\ \quad + (\Re_2 + \Re_4).(\Phi_1 - \Phi_3) \\ 0 = (\Re_2 + \Re_4).(\Phi_1 - \Phi_3) - (\Re_3 + \Re_{\theta 3} + \Re_4).\Phi_3 \\ \quad + (\Re_5 + \Re_{\theta 5}).(\Phi_1 - \Phi_2 - \Phi_3) \end{cases} \quad (2)$$

After rewriting, one can find the matrix formulation:

$$\overline{NI} = [\Re_\theta].\overline{\Phi} \quad (3)$$

with the following position dependant reluctance matrix:

$$[\Re_\theta] = \begin{bmatrix} \Re_1 + \Re_{\theta 4} & 0 & \Re_3 + \Re_{\theta 3} + \Re_4 \\ \Re_2 + \Re_4 & \Re_{51} + \Re_{\theta 51} & -(\Re_2 + \Re_3 + 2\Re_4 + \Re_{\theta 3}) \\ \Re_2 + \Re_4 + \Re_5 + \Re_{\theta 5} & -(\Re_5 + \Re_{\theta 5}) & -(\Re_2 + \Re_3 + 2\Re_4 + \Re_{\theta 3} + \Re_5 + \Re_{\theta 5}) \end{bmatrix} \quad (4)$$

The constant reluctances can be expressed as:

$$\Re_i = \frac{l_i}{\mu_0 . \mu_r . A_i} \quad (5)$$

The position dependant reluctances can be approximated for small angles of θ as:

$$\Re_{\theta 3} \approx \frac{\theta . l_6}{\mu_0 . A_3} \quad \Re_{\theta 4} \approx \frac{\theta . l_4}{\mu_0 . A_1}$$
$$\Re_{\theta 5} \approx \frac{2.\theta . l_4}{\mu_0 . A_5} \quad \Re_{\theta 51} \approx \frac{2.\theta . l_4}{\mu_0 . A_{51}} \quad (6)$$

The magnetic torque is obtained by derivation of the magnetic co-energy with respect to the position:

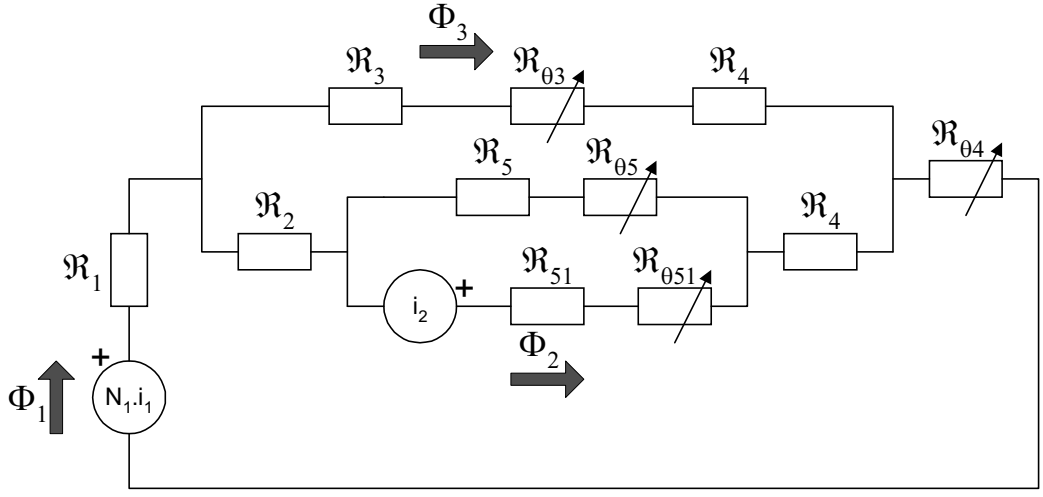

Fig. 4 Equivalent magnetic circuit

$$T_m = -\frac{\partial W_m}{\partial \theta} = -\frac{\partial}{\partial \theta}\left(\frac{1}{2}.\overline{\Phi}^t.[\Re_\theta].\overline{\Phi}\right) = \frac{1}{2}.\overline{\Phi}^t.\frac{\partial[\Re_\theta]}{\partial \theta}.\overline{\Phi} \quad (7)$$

The mechanical equation, defining the motion of the relay can be written as:

$$\frac{d^2\theta}{dt^2} = \frac{1}{J}.\left(T_m + T_g - T_s - T_d\right) \quad (8)$$

with: J = inertia of moving part [kg.m²]
T_m = magnetic torque [N.m]
T_g = gravitational torque [N.m]
T_s = spring torque [N.m]
T_d = damping torque [N.m]

The gravitational torque is constant and equals:

$$T_g = M.g.l_4 \quad (9)$$

with M the mass of the moving part [kg]

Spring and damping torque can be expressed as a function of respectively θ and dθ/dt:

$$T_s = c_t.(\theta_0 - \theta)$$
$$T_d = -D.\frac{d\theta}{dt} \quad (10)$$

with c_t the torsional spring constant [N.m/rad] and D the damping factor [N.m.s/rad]

4. MATLAB®/SIMULINK SOLVING

The equations (3) to (10) are discretised and solved with Matlab®/Simulink. At every sample time (T_s = 20 µs), a new position dependant reluctance matrix is calculated.

The modeled and tested device is an undervoltage relay 220…240V, 50Hz.

Fig. 5 shows the simulation results. It includes the visualization of current, flux and torque. In the flux versus time diagram of fig. 5b, the phase shift of Φ_2 with respect to Φ_1 is clearly visible. At rising shading ring flux, the resulting magnetic torque (fig. 5c) halts touching the zero value line. This results in a damping of the relay bouncing at double frequency. Fig. 6 shows the position of the moving relay part, due to the interaction of magnetic torque and spring torque. Also the damping influence of the shading ring is represented.

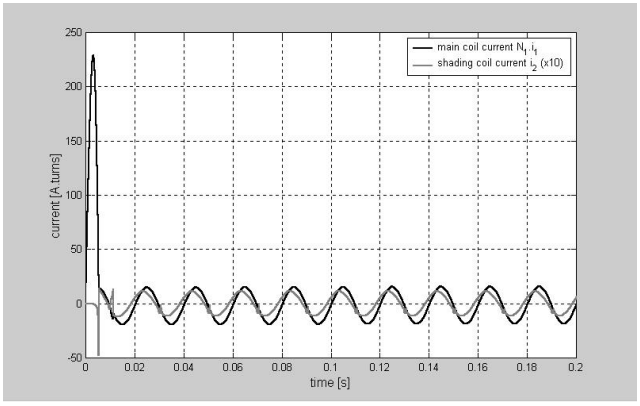

Fig. 5a Current Ni [ampère.turns]

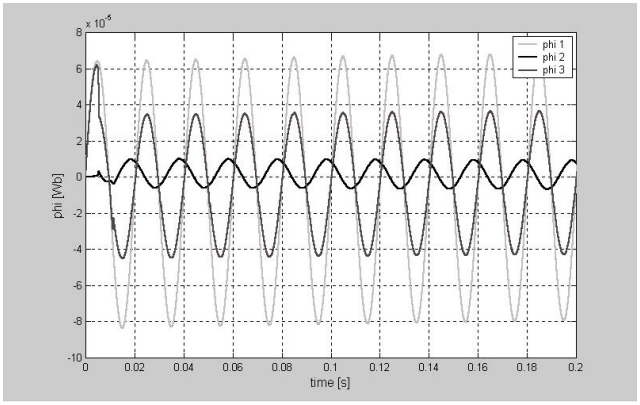

Fig. 5b Flux Φ [Wb]

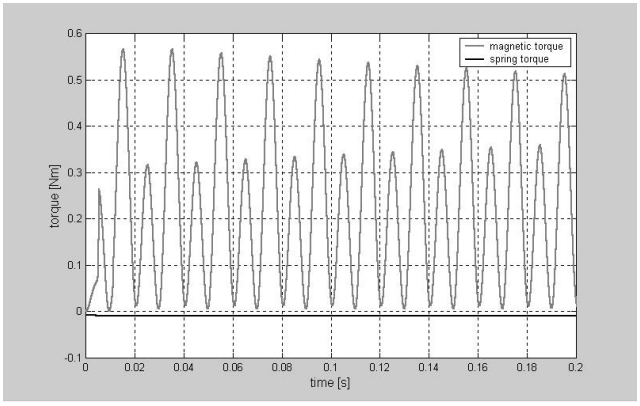

Fig. 5c Magnetic torque and spring torque [Nm]

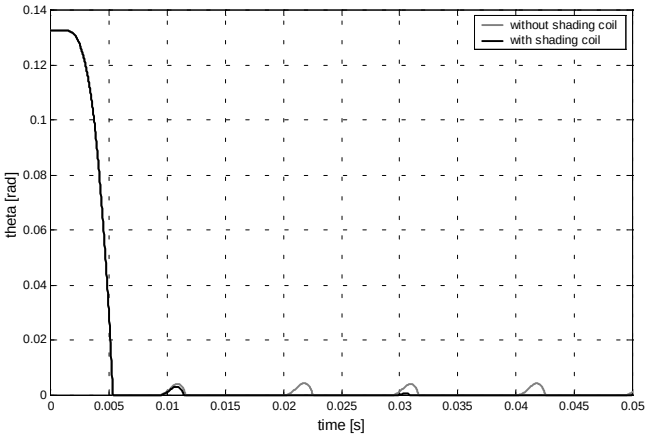

Fig. 6 Position angle of moving part [rad]

5. VOLTAGE TOLERANCE CURVES

An experimental test set-up is build using a programmable power source as dipgenerator. The source switches synchronously from mains (230V, 50Hz) to a programmed source. Several voltage dips of various magnitude, duration and point-on-wave are applied to the undervoltage relay. Fig. 7 shows the measured voltage tolerance curves.

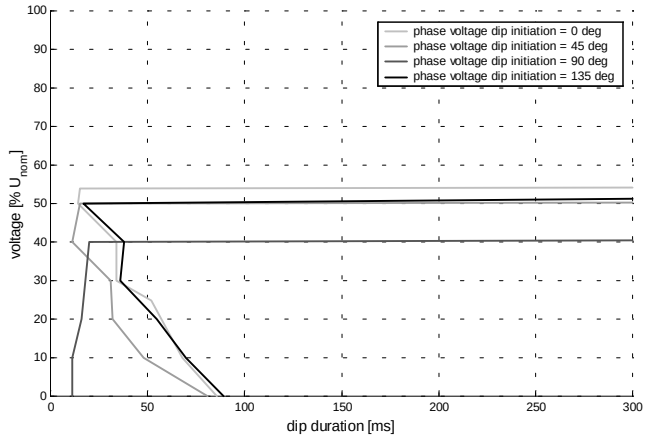

Fig. 7 Voltage tolerance curves (measured)

The shape of the curves highly depends on the point-on-wave of the voltage dip. The previously described model is used to explain the phase-dependant behavior of the undervoltage relay. At a point-on-wave of 90 degrees, the voltage waveform is at its maximum value while the flux waveform (Φ_1 and Φ_3) is at its minimum. This results in a minimum of magnetic energy needed to pass the voltage dip (11ms for a dip of 0% remaining voltage). Fig. 8 shows the simulation of the voltage, flux and torque waveforms during a voltage dip (phase angle = 90 deg.).
From the voltage tolerance curves of Fig. 7 it can be seen that, for a point-on-wave of 0 degrees, the relay is much more sensitive to voltage dips (e.g. 50% U_{rated}) than to short interruptions (0% U_{rated}). Using the proposed simulation model, the behavior during a voltage dip and interruption is represented in Fig. 9a and 9b.

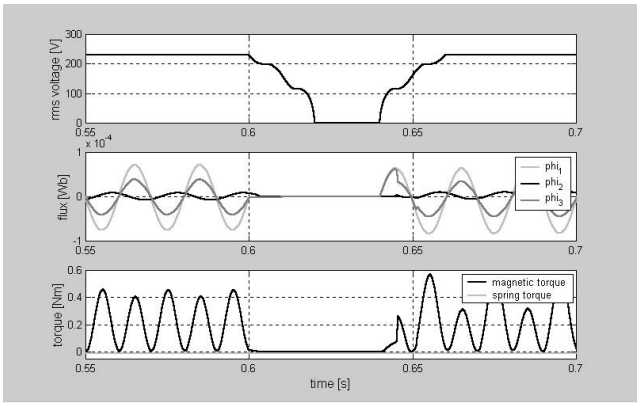

Fig. 8 Voltage (rms), flux and torque waveform during voltage interruption of 40 ms (phase angle = 90 deg.)

During the voltage dip of 50% U_{rated} (Fig. 9a), a lower magnetic flux is forced into the system. This pulsating magnetic energy, however, results in a lack of magnetic force and a very low dip surviving time (Fig. 9a). During an interruption (0% U_{rated}), there is no alternating magnetic flux forced into the relay. The magnetic energy, being at its maximum, can gradually decrease and results in a much larger dip survival time (Fig. 9b).

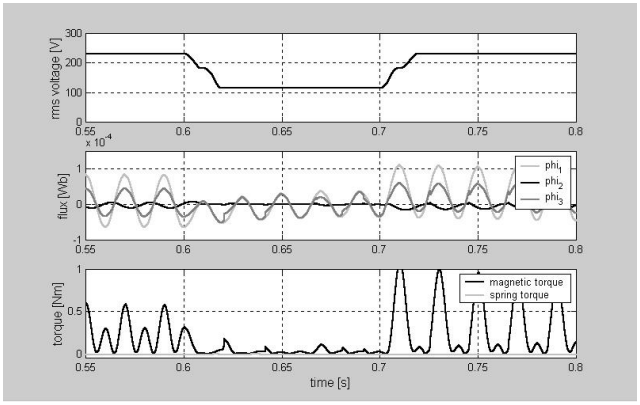

Fig. 9a Voltage (rms), flux and torque waveform during voltage dip (50% U_{nom}) of 100 ms (phase angle = 0 deg.)

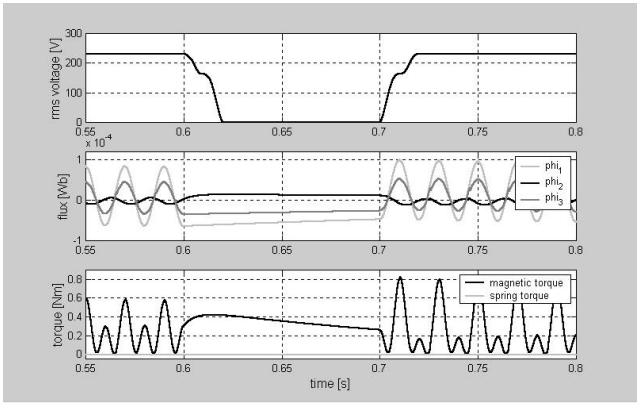

Fig. 9b Voltage (rms), flux and torque waveform during voltage interruption of 100 ms (phase angle = 0 deg.)

6. MODEL CONSTRAINTS

The linear model does not include local saturation nor hysteresis of the core material. This can be implemented using a look-up table or polynomial function. An improved model can also be realized using FE-techniques (2-D or 3-D) [3]. However, one has always to consider whether the improvements in model accuracy still add a similar value to the desired model results.

7. GLOBAL MACHINE IMMUNITY

Adding an undervoltage relay in order to protect parts of the machine towards overcurrents after a voltage interruption can highly reduce the immunity towards short voltage dips. This can be visualized (figure 10) by superposing the voltage tolerance curve of the system (e.g. weaving machine) with the voltage tolerance curve of the undervoltage relay. Especially when efforts are made in the DC-link of the drive (capacitor battery, boost converter, kinetic buffering, …) to improve the voltage dip immunity, one has to consider the effect of adding electromagnetic elements, such as undervoltage relays at the machine mains.

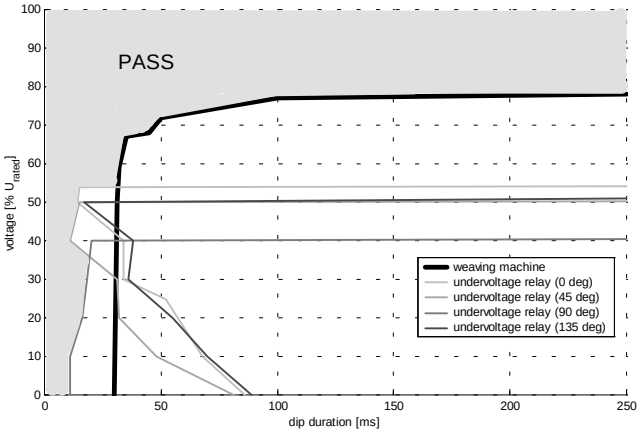

Fig. 10 Voltage tolerance curves (measured)

8. CONCLUSION

The behaviour of AC undervoltage relays during voltage dips highly depends on the point-on-wave of the dip initiation. The model, based on electrical, magnetic and mechanical equations, is validated, based on the measured voltage tolerance curves. This knowledge of voltage tolerance curves is very important to define the dip immunity of the component. The voltage dip immunity of a machine, which is the assembly of different components, is defined by the immunity of the weakest component. As a result, the machine dip immunity can be found as the enveloped voltage tolerance curve of all considered components, such as undervoltage relays, contactors, variable speed drives (VSD), … This finally results in the knowledge of the complete machine behavior under voltage dip conditions.

9. ACKNOWLEDGEMENT

The authors wish to thank the Flemish Government for granting the project 'Invloed van spanningsdips bij snelheidsgeregelde aandrijvingen' (IWT-HOBU).

REFERENCES

Proceedings Papers:

[1] F. Córcoles, J. Pedra, J.P. Garrido and R. Baza, Model for the dynamic study of AC contactors, *Proc. ICEM 2000*, Espoo, Finland, pp. 449-453.

[2] K. Stockman, F. D'hulster, K. Verhaege, J. Desmet and R. Belmans, Voltage dip immunity test set-up for induction motor drives, *Proc. 11th international symposium on power electronics Ee 2001*, Novi Sad, Yugoslavia, pp. 303-307.

[3] X. Alabern, R. Mujal, G. Figa-Tena, 2-D Finite element analysis of magnetic pull force for a real AC electromagnetic contactor, *Proc. ICEM 2000*, Espoo, Finland, pp. 454-457.

[4] E. Randolph Collins, Jr. and Michael A. Bridgwood, The impact of power system disturbances on AC-coil contactors, *Proc. IEEE Textile, fiber and film industry technical conference*, 1997, pp. 2-8.

Journal Papers:

[5] P.I. Kolterman, J.P. Assumpçao Bastos and S.R. Arruda, A model for dynamic analysis of AC contactor, *IEEE transactions on Magnetics*, vol. 28, no. 2, march 1992, pp.1348-1350.

Books:

[6] M.H.J. Bollen, *Understanding power quality problems: Voltage sags and interruptions* (New Jersey: IEEE Press, 2000).

[7] Chee-Mun Ong, *Dynamic simulation of Electric Machinery using Matlab®/Simulink* (New Jersey: Prentice Hall PTR, 1998).